Electronic Supporting Information

Serum fingerprinting by slippery liquid-infused porous SERS for non-invasive lung cancer detection

Chenlei Cai,[a,†] Yujie Liu,[b,†] Jiayu Li,[a] Lei Wang*[a] and Kun Zhang*[b]

a. Department of Medical Oncology, Shanghai Pulmonary Hospital, Tongji University School of Medicine, Shanghai, 200433 China.

b. Shanghai Institute for Pediatric Research, Shanghai Key Laboratory of Pediatric Gastroenterology and Nutrition, Xinhua Hospital, Shanghai Jiao Tong University School of Medicine, Shanghai 200092, China.

†Chenlei Cai and Yujie Liu contributed equally to this work.

*Corresponding author

E-mail: wangleixxxn@163.com; kunzhang@shsmu.edu.cn

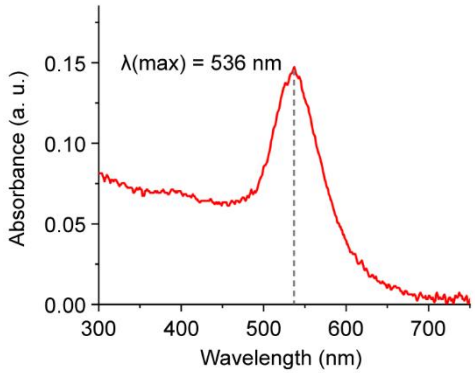

Fig. S1 UV-vis absorption spectrum of Au NPs determined on a Nanodrop 2000 spectrophotometer.

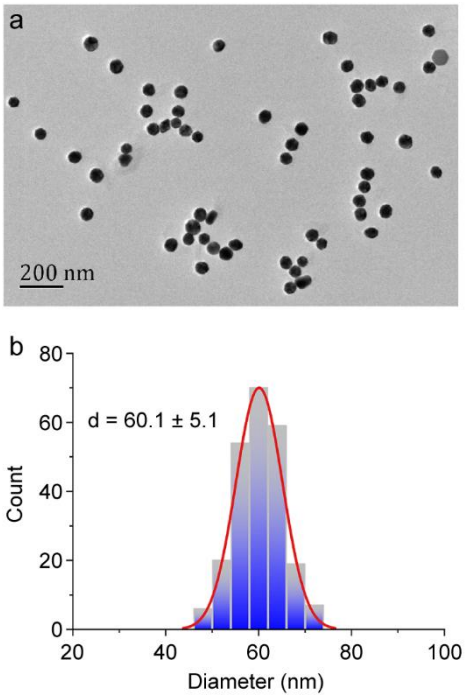

Fig. S2 (a) TEM image of Au NPs. (b) Size distribution of Au NPs estimated from the SEM result.

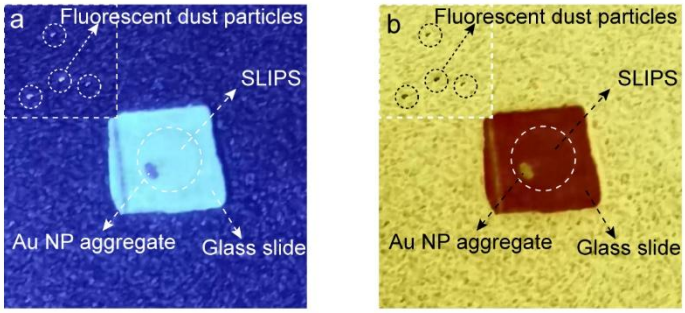

Fig. 3 (a) Photograph of Au NP aggregate formed by evaporating Au NP solution containing 0.02 mM of methylene blue under 365 nm UV irradiation. (b) Color inversion mode of the photograph in (a). Insert at the left-up corner showing the fluorescent dust particles at the desk surface. These fluorescent dusts were used as the luminescent references. From the above photographs, especially the picture b, we observed no apparent photoluminescence at the SLIPS after droplet evaporation, indicating high efficiency of sample collection of the SLIP substrate.

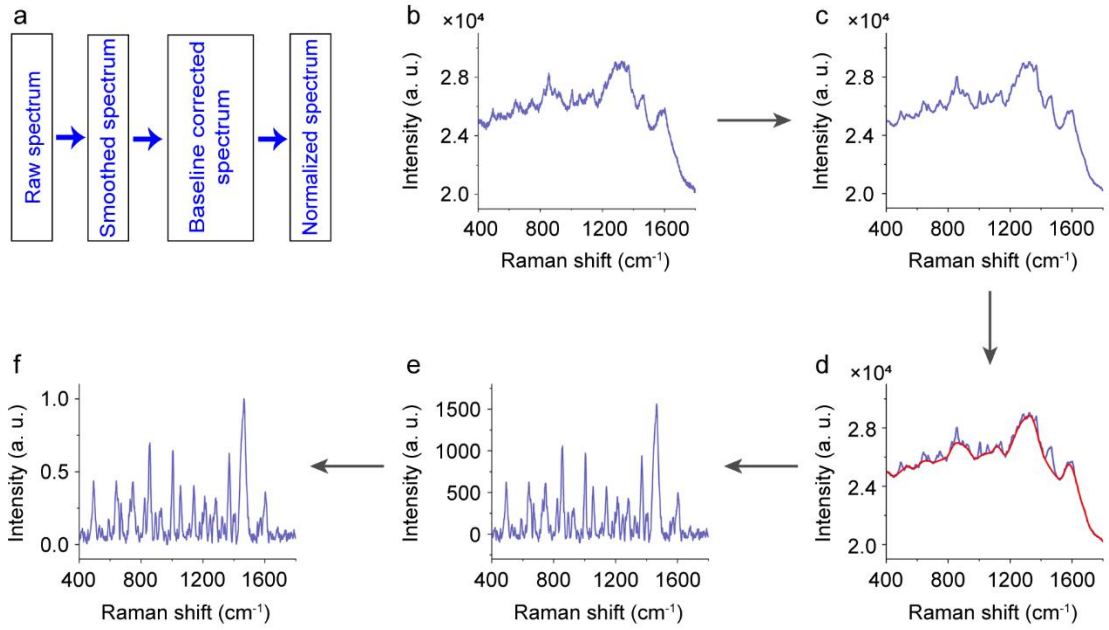

Fig. S4 (a) Pipeline of SERS spectral preprocessing. (b) A Raw SERS spectrum. (c) The smoothed spectrum. For reproducibility, the raw spectrum was first subjected to cosmic ray removal and then denoised by the Savitzky-Golay algorithm (polynomial order 3, points of window 11). (d) Baseline correction using the Asymmetric least-squares algorithm (asymmetric factor 1×10^{-3}, threshold 0.075, iteration number 10). (e) The baseline-corrected spectrum. (f) The min-max normalized spectrum.

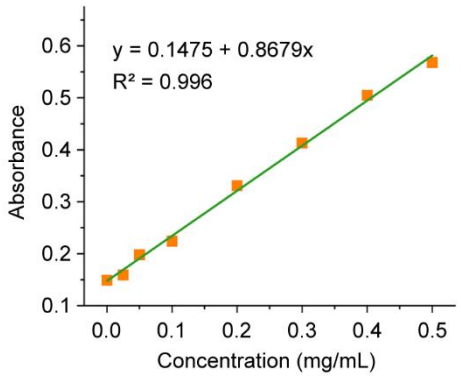

Fig. S5 Calibration curve for BCA testing of the serum protein concentration.

The protein concentration of the ultrafiltration (Millipore, 3 KD)-treated serum was tested with the bicinchoninic acid (BCA) Protein Assay kit (Biyuntian, China) according to the manufacturer's Instruction. From the calibration curve in **Fig.** S5, we measured that the protein concentrations of the serum samples were in the range of 0.019 to 0.031 mg/mL, three orders of magnitude lower than normal physiological values (60 to 120 mg/mL). The result indicates that some low-abundance low-molecular-weight proteins are retained in the samples, although the large, high-abundance proteins such as HAS (66 KD) has been removed. We infer that these small proteins and the serum polypeptides may contribute to the amide vibrational modes in the SERS spectra.

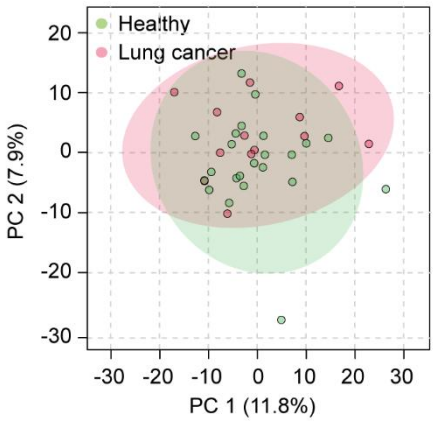

Fig. S6 PCA of SERS data of serum samples from 13 healthy controls and 23 lung cancer patients.

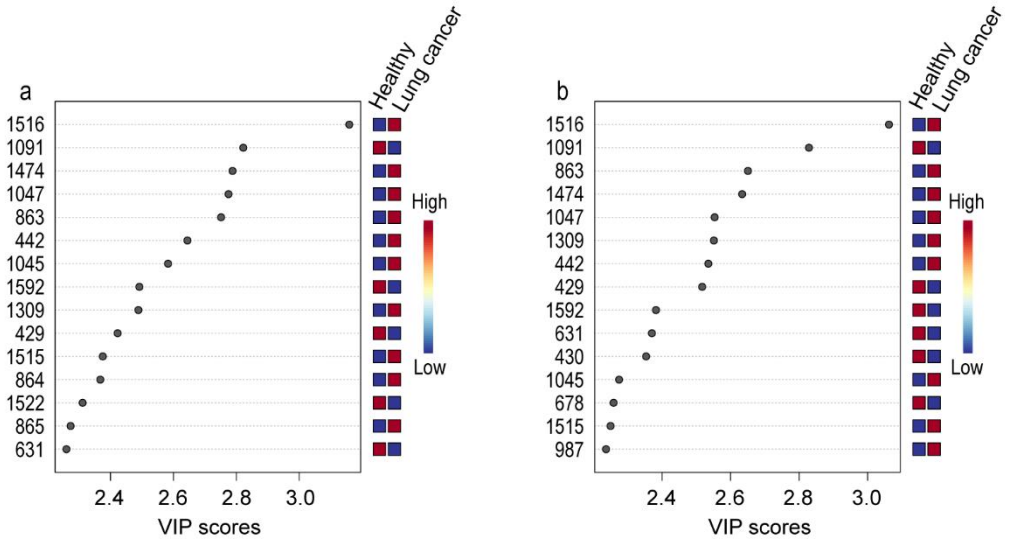

Fig. S7 Significant SERS features identified by (a) PLS-DA and OPLS-DA from serum samples from the 10 healthy controls and 20 lung cancer patients.

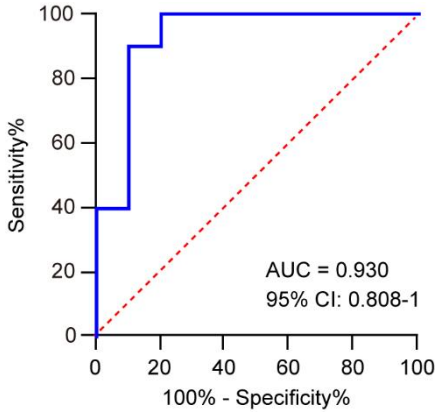

Fig. S8 Receiver operating characteristic (ROC) curve of classification mode for the validation data.

Table S1 SLIPSERS peak positions and assignments of vibrational modes of methylene blue

Peak position (cm^{-1})	Vibrational mode	Peak position (cm^{-1})	Vibrational mode
445	df(C-N-C)	1183	s(C-N)
505	df(C-N-C)	1305	s(C–C) ring
598	df(C-S-C)	1330	b(C-H) in-plane
674	b(C-H) out-of-plane	1394	as(C-N)
774	b(C-H) out-of-lane	1441	as(C-N)
894	b(C-H) out-of-plane	1469	s(C–C) ring
1041	b(C-H) in-plane	1505	as(C-C)
1158	b(C-H) in-plane	1625	s(C–C) ring, s(C-N-C)

Abbreviations:

b: bending, df: skeletal deformation, s: stretching, as: asymmetric stretching

Band assignments are based on references [S1], [S2], and [S3].

Table S2 Serum SLIPSERS peak positions and tentative assignments of vibrational modes

Peak position (cm^{-1})	Vibrational mode	Tentative assignments
494	/	L-Arginine, guanine, polysaccharides
591	/	Amide IV, uric acid
640	t(C-C)	L-Tyrosine, lactose
747	rv	Thymine
823	rb	Tyrosine
855	rb	Tyrosine
893	b(C-O-H)	D-Galactosamine
928	s(C-C)	Proline, valine
1003	s(C-C), rb(C-C)	Phenylalanine
1029	b(C-H)	Phenylalanine
1054	s(C-C, C-O)	Glycogen, lipids
1137	s(C-N), ss(C-H)	D-Mannose
1181	ss(C-O, C-C)	Carbohydrates
1213	s(C-N), b(N-H)	Amide III (β-pleated sheet)
1244	s(C-N)	Nucleic acid
1289	α-helix	Amide III (α-helix)
1372	/	Adenine, thymine
1461	b(C-H)	Disaccharides
1576	s(C=C)	Phenylalanine, acetoacetate, riboflavin
1600	s(C=C)	Phenylalanine
1678	s(C=C)	Amide I (β-pleated sheet)

Abbreviations:

b: bending, rb: ring breathing, rv: ring vibration, s: stretching, ss: symmetric stretching, t: twist

Band assignments are based on references [S1], [S2], [S3], [S4], [S5], [S6] [S7], [S8], and [S9].

Table S3 Baseline characteristics of patients and healthy controls

	Cancer	Control	
Patient characteristics	(n = 33)	(n = 23)	P
Age (years; IQR)	65 (56-68)	59 (55-63)	0.135
Gender			
Male (%)	25 (76%)	16 (70%)	0.761
Female (%)	8 (24%)	7 (30%)	
Histology			
Adenocarcinoma (%)	23 (70%)	NA	NA
Squamous cell (%)	7 (21%)	NA	
Other	3 (9%)	NA	
Stage			
I (%)	2 (6%)	NA	NA
II (%)	2 (6%)	NA	
III (%)	10 (30%)	NA	
IV (%)	19 (58%)	NA	
Smoking history			
Yes (%)	23 (70%)	NA	NA
No (%)	10 (30%)	NA	

Abbreviations:

IQR, interquartile range; NA, nonapplicable.

References

S1 X. Dong, H. Gu, J. Kang, X. Yuan, and J. Wu, *Colloids Surf., A,* 2010, **368**, 142-147.

S2 G.-M. Xiao, and S.-Q. Man, *Chem. Phys. Lett.*, 2007, **447**, 305-309.

S3 S. H. de Araujo Nicolai, P. R. P. Rodrigues, S. M. LAgostinho, and J. C. Rubim, *J. Electroanal. Chem.*, 2002, **527**, 103-111.

S4 X. Lin, D. Lin, Y. Chen, J. Lin, S. Weng, J. Song, and S. Feng, *Adv. Funct. Mater.*, 2021, **31**, 2103382.

S5 H. Li, S. Zhang, R. Zhu, Z. Zhou, L. Xia, H. Lin, and S. Chen, *Spectrochim. Acta, Part A*, 2022, **278**, 121314.

S6 R. Xiao, X. Zhang, Z. Rong, B. Xiu, X. Yang, C. Wang, W. Hao, Q. Zhang, Z. Liu, C. Duan, K. Zhao, X. Guo, Y. Fan, Y. Zhao, H. Johnson, Y. Huang, X. Feng, X. Xu, H. Zhang, and S. Wang, *Nanomedicine*, 2016, **12**, 2475-2484.

S7 L. Shao, A. Zhang, Z. Rong, C. Wang, X. Jia, K. Zhang, R. Xiao, and S. Wang, *Nanomedicine*, 2018, **14**, 451-459.

S8 V. Moisoiu, A. Stefancu, D. Gulei, R. Boitor, L. Magdo, L. Raduly, S. Pasca, P. Kubelac, N. Mehterov, V. Chiș, M. Simon, M. Muresan, A. I. Irimie, M. Baciut, R. Stiufiuc, I. E. Pavel, P. Achimas-Cadariu, C. Ionescu, V. Lazar, V. Sarafian, I. Notingher, N. Leopold, and I. Berindan-Neagoe, *Int. J. Nanomedicine*, 2019, **14**, 6165-6178.

S9 X. Zheng, G. Wu, J. Wang, L. Yin, and X. Lv, Biomed. *Opt. Express*, 2022, **13**, 1912-1923.

S10 J. Lei, D. Yang, R. Li, Z. Dai, C. Zhang, Z. Yu, S. Wu, L. Pang, S. Liang, and Y. Zhang, *Spectrochim. Acta, Part A*, 2021, **261**, 120021.

S11 Z. Wang, Y. Hong, H. Yan, H. Luo, Y. Zhang, L. Li, S. Lu, Y. Chen, D. Wang, Y. Su, and G. Yin, *Spectrochim. Acta, Part A*, 2022, **279**, 121483.

S12 K. Liu, S. Jin, Z. Song, L. Jiang, L. Ma, and Z. Zhang, *Vib. Spectrosc.*, 2019, **100**, 177-184.